

Baby Got Back?

An Analysis of Front-Facing Representations of Orientable Surfaces

Jonathan Kelner
Christopher Mihelich

May 27, 2001

1 Introduction

When manipulating a surface in computer graphics, one frequently begins by triangulating it with one-sided triangles; he then often restricts his attention to the triangles whose front sides can be seen from a given vantage point. As such, many algorithms only concern themselves with “front-facing” subsets of the original surface. However, to date relatively little analysis has been performed of the topological and geometric properties of these front-facing surfaces. That is the task that we take up in this paper.

There are two settings in which one can examine the topology of front-facing surfaces. First, one can investigate the properties of front-facing surfaces as abstract topological spaces. This turns out to be easy, and it admits a very simple and complete description. Alternatively, one can consider front-facing surfaces as objects embedded in \mathbb{R}^3 and examine their properties with respect to smooth deformations. This is considerably more subtle and complex, and the effect of requiring a surface to be front-facing in this context is a good deal less transparent. Nonetheless, it is still possible to carry out a complete analysis of front-facing surfaces in this setting, and we provide it in the sequel.

Our analysis requires some ideas from topology that lie outside the standard corpus of computer graphics literature. Both in order to keep our paper self-contained, and because we believe they may be fruitfully applied to other questions in computer graphics, we begin in section 2.2 by providing a brief treatment of these topological prerequisites.

In section 3 we provide a rigorous definition of front-facing surfaces, and we then show that the abstract topological spaces that can be realized as front-facing surfaces are precisely the oriented surfaces with boundary. These are fully enumerated and described in section 2.2, so this will provide a complete understanding of the topological properties of (unembedded) front-facing surfaces.

In section 4, we shall define the *spine* of a front-facing surface, which will be our main tool for understanding front-facing surfaces embedded in \mathbb{R}^3 . We shall then use this to put equivalence classes of embedded front-facing surfaces up to smooth deformation into a one-to-one correspondence with certain one-dimensional objects. These one-dimensional objects will then illuminate the essential structure of an embedded front-facing surface.

In section 5, we shall derive as a corollary to the construction in the previous section the statement that *any* embedded orientable surface with boundary can be deformed to be front-facing. This will thus show the requirement that a surface be front-facing to be a very weak one. It will simultaneously allow the analysis in the preceding section to apply to all orientable surfaces with boundary.

In section 6, we shall consider the boundary of a front-facing surface and in particular show how to use just the boundary of a front-facing surface to compute the genus of the surface, which cannot be done without the front-facing presentation. This will be done using the concept of winding numbers.

Finally, in section 7, we shall deviate slightly from front-facing surfaces and use the topological tools discussed earlier in the paper to give an algorithm to “cut” a surface with boundary so that it becomes topologically a disk. The algorithm that we provide is linear in the number of triangles in the surface, and it uses the minimal number of cuts.

2 Utilitarian Introduction to Topology

In computer graphics, the usual concept of shape is laden with geometrical specifics: positions, lengths, and so forth. It is often of interest, however, to consider a somewhat more flexible notion of shape than the strict notion of congruence (or the stricter notion of coincidence) in \mathbb{R}^3 . The geometrical difference between two spheres of radii one inch and one yard respectively is certainly significant if you are rendering one in a video game or trying to carry one up a hill, but both have “the same shape” in some sense: we call them both spheres, after all. What exactly does “sphere” mean to us? In fact, our intuitive notion of a sphere is fairly broad, encompassing objects that, strictly speaking, are not spheres at all. We would say that the surface of a golf ball is a sphere, despite its many indentations. To human intuition the golf ball “looks like a sphere” except for its surface detail; but that phrase is not an analytically precise notion.

The mathematical discipline of topology, often characterized as the study of abstract shape, defines with analytical precision a variety of properties that make concrete and exact the intuitive notion that two objects do or do not “look alike” and provides powerful tools for analyzing shape in this fairly amorphous setting. In this section we introduce certain fundamental concepts and theorems of topology of which we shall have frequent use later.

2.1 Notions of equivalence

Topologists have several ideas of what it means for two shapes to be equivalent, each of which is preferable to its alternatives in appropriate settings. We introduce three of these notions here.

Homeomorphism. The most stringent notion of equivalence used in topology is that of *homeomorphism*. Intuitively, two shapes are homeomorphic if you can transform one into the other by stretching, squishing, dilating, or otherwise pulling parts of the shape around as if it were composed of uncommonly flexible putty. You are *not* allowed to tear the shape, to smash regions out of existence, or to paste points or regions together.

Of course, a mathematician cannot work with such hand-waving. A precise definition is the following:

Definition 2.1 *Let $A \subset \mathbb{R}^m$ and $B \subset \mathbb{R}^n$ be subsets of Euclidean spaces of some dimensions. A function $f : A \rightarrow B$ is called a homeomorphism if*

1. *f is one-to-one and onto;*
2. *f is continuous; and*
3. *the inverse function f^{-1} is continuous.*

Sets A and B for which such an f exists are called homeomorphic or topologically equivalent.

Condition 1 means that no points were created or destroyed by the transformation, and condition 2 means that the transformation did not tear A . Condition 3 is needed to prevent the transformation from joining disconnected regions of A , as the following example shows. Let $A \subset \mathbb{R}^1$ be the union of the half-open intervals $[0, 1)$ and $[2, 3)$, and let $B \subset \mathbb{R}^1$ be the interval $[0, 2)$. Define $f : A \rightarrow B$ by the rule

$$f(t) = \begin{cases} t, & \text{if } 0 \leq t < 1; \\ t - 1, & \text{if } 2 \leq t < 3. \end{cases}$$

Then f is a continuous bijection and so satisfies conditions 1 and 2, but the spaces A and B do not look alike—the former has more “pieces” (topologists call them *connected components*) than the latter. In fact f is not a homeomorphism because it violates condition 3: the inverse function $f^{-1} : B \rightarrow A$, namely

$$f^{-1}(s) = \begin{cases} s, & \text{if } 0 \leq s < 1; \\ s + 1, & \text{if } 1 \leq s < 2, \end{cases}$$

is not continuous at $s = 1$.

Returning to the sphere example, we can see now that the definition of homeomorphism declares all of the examples of “spheres” above to be topologically equivalent. Consider the spheres of radii one inch and one yard, both centered at the origin of \mathbb{R}^3 . The continuous function

$$(x, y, z) \mapsto (36x, 36y, 36z)$$

of multiplication by 36 maps the small sphere onto the large one in a one-to-one fashion, and its obvious inverse

$$(x, y, z) \mapsto \left(\frac{1}{36}x, \frac{1}{36}y, \frac{1}{36}z\right)$$

is continuous. Consequently the two spheres are homeomorphic. We can prove that any two spheres in \mathbb{R}^3 , of any radii, centered at the origin are homeomorphic by replacing 36 in the above argument by the ratio of the two radii. If we replace the dilation by a more general affine transformation, we can prove any two spheres, concentric or not, to be homeomorphic.

The surface G of the golf ball requires a more complicated construction. We draw a sphere S surrounding and concentric with the golf ball; call the common center C . A homeomorphism $f : G \rightarrow S$ may be defined by radial projection: for each $x \in G$ let $f(x)$ be the point at which the ray from C through x intersects S (see Figure 1). This is a continuous bijection, and f^{-1} is continuous. To be entirely proper, we should describe precisely the shape of a golf ball and prove the asserted properties of f and f^{-1} in detail; the required formulae, however, would be messy and unenlightening, and in fact topologists routinely omit such verifications, so we will do the same.

Homotopy equivalence. For two spaces A and B to be homeomorphic, there must be a pair of continuous functions $f : A \rightarrow B$ and $g : B \rightarrow A$ such that the compositions $g \circ f$ and $f \circ g$ are the identities on A and B respectively (that is, we have $g = f^{-1}$). The less strict notion of *homotopy equivalence* of A and B requires instead that functions f and g exist such that $g \circ f$ and $f \circ g$ may be continuously deformed to the identities on A and B respectively (this time f and g need not be inverse functions, but in this setting we call them *homotopy inverses*). In general, a *homotopy* or continuous deformation between two maps $h_0, h_1 : X \rightarrow Y$ is a continuous map $h : X \times [0, 1] \rightarrow Y$ such that $h(\cdot, 0) = h_0$ and $h(\cdot, 1) = h_1$; if such an h exists, we say that h_0 and h_1 are homotopic, and h is a homotopy between them. Usually we write the parameter in $[0, 1]$ as a subscript, so that $h(x, t)$ appears as $h_t(x)$.

An important special case of homotopy equivalence is obtained from a *deformation retraction* of a space X onto a subset $A \subset X$, which is defined to be a homotopy $h : X \times I \rightarrow X$ such that

h_0 is the identity on X , but the image of h_1 lies entirely in A , and moreover each slice h_t fixes every point in A . Conceptually, such a homotopy is just a means of compressing X onto A without moving A at all. We claim that the final map $h_1 : X \rightarrow A$ is a homotopy equivalence of X with A , which we shall prove by showing that the inclusion $i : A \rightarrow X$ is a homotopy inverse for h_1 . On one hand, the composition $h_1 \circ i$ is exactly the identity on A because h_1 fixes every point of A . On the other hand, the composition $i \circ h_1$ is just h_1 , which is homotopic to the identity on X via h .

Obviously any homeomorphism is a homotopy equivalence. A simple example of a homotopy equivalence that is not a homeomorphism is obtained by taking X to be the interval $[-1, 1]$ and A to be the point 0 and defining a deformation retraction h of X onto A by the formula $h_t(x) = (1-t)x$. Then h_1 , the zero map, is a homotopy equivalence, so $[-1, 1]$ is homotopy-equivalent to a point; but the interval and the point are clearly not homeomorphic because there is no bijective function between them, much less a bijection continuous in both directions. The same formula for h can be used to show that any convex set in a Euclidean space is homotopy-equivalent to a point. Spaces that are homotopic to a point in this fashion are called *contractible*.

Isotopy. Sometimes the strict notion of homeomorphism is not strict enough. Homeomorphism is a relationship between abstract topological spaces; even if the topological spaces we care about happen to be subsets of, say, a Euclidean space, the notion of homeomorphism completely ignores the manner in which the spaces are embedded in the Euclidean space. The benefits of the abstract treatment have been discussed already. In certain cases, however, the loss of information is undesirable. For instance, consider the two pairs of circles in \mathbb{R}^3 depicted below (the general term for a finite collection of disjoint circles in \mathbb{R}^3 is *link*). As abstract topological spaces, the two links are homeomorphic—each is a disjoint union of two circles. But as objects in three-dimensional space, the two links do not deserve to be considered equivalent. No amount of pushing, pulling, and stretching in \mathbb{R}^3 will unlink the circles in the second picture. Thus, although the pairs of circles can be transformed into each other abstractly, the transformation cannot be performed by fiddling around in the ambient space \mathbb{R}^3 .

The notion of *isotopy* is a variant of homeomorphism that preserves information about the embedding. Formally, two spaces A and B , contained in a larger space C , are called *isotopic in C* if there is a homotopy $h : A \times [0, 1] \rightarrow C$ so that

1. the slice h_0 is the inclusion $A \rightarrow C$;
2. the slice h_1 is a homeomorphism of A onto B ; and
3. each intermediate slice h_t is a homeomorphism of A onto its image.

Condition 3 is what gives the concept of isotopy its greater strictness; it means essentially that you may not squeeze all or part of A down to a point and then rematerialize it elsewhere. For instance, in Figure 2, which shows the Euclidean plane with all but one point of the line $y = 0$ excised, the two circles are homeomorphic, and there is a homotopy satisfying conditions 1 and 2 above, but the circles are not isotopic: you can't fit one circle through the narrow hole without smashing points together.

2.2 Piecewise-linear objects

Arbitrary spaces and arbitrary continuous maps can be fairly difficult to analyze, so it is convenient to introduce a restricted class of spaces and maps with more tractable behavior. The basic building block for one of these restricted spaces is the n -dimensional *simplex* (for $n \geq 0$), which is the convex

hull of $n + 1$ points in general position in \mathbb{R}^n . For $n = 0, 1, 2,$ and $3,$ an n -simplex is a point, a line segment, a triangle, or a tetrahedron respectively. The *faces* of a simplex are the convex hulls of all proper subsets of its vertex set. In the case of a 3-simplex (tetrahedron), the faces are the vertices and edges as well as the ordinary (two-dimensional) faces.

We now define a *simplicial complex* to be a finite union of simplices such that any two simplices in the complex intersect in the empty set or a single simplex. The intersection condition rules out anomalous intersections such as those in Figure 3, which would complicate many arguments unnecessarily. The *dimension* of a simplicial complex is the largest dimension of a simplex appearing in it. The case of a 2-dimensional complex is a concept very familiar in computer graphics: it is merely a triangular mesh (often irregular and not a manifold, however). We shall generally restrict our attention to simplicial complexes hereafter. We shall also generally consider only *piecewise linear* maps, namely, maps for which the domain space can be partitioned into several regions so that the restriction of the map to each region is an affine function. As an example, a piecewise-linear embedding of the circle in the Euclidean plane must have a polygonal rather than a smooth image.

For finite simplicial complexes K we can define the *Euler characteristic* $\chi(K)$, a numerical invariant of profound importance. If K has n_0 vertices, n_1 edges, n_2 two-dimensional faces, and so forth, the Euler characteristic is defined by the formula

$$\chi(K) = n_0 - n_1 + n_2 - n_3 + \cdots$$

(because K is finite we have $n_j = 0$ for large j , whence the sum breaks off after finitely many terms). If K is a 1-dimensional complex, a graph with vertex set V and edge set E , say, then we have $\chi(K) = |V| - |E|$. For a surface with faces F we have $\chi(K) = |V| - |E| + |F|$, which is the case of the formula that we shall most often need.

It can be proven that $\chi(K)$ is a topological invariant, i.e., that if K and K' are homeomorphic complexes, then $\chi(K) = \chi(K')$. Thus χ does not depend on the choice of a simplicial-complex structure on a space. More generally, if K and K' are merely *homotopy-equivalent* complexes, we still have necessarily that $\chi(K) = \chi(K')$. We leave the proof of these facts to any reputable text on algebraic topology.

2.3 The Topology of Orientable Surfaces

Since they are our primary object of study, we briefly review the topology of orientable surfaces. For a more complete treatment, see [1].

For the sake of this paper, a *surface* will be taken to be a compact 2-manifold, possibly with boundary. If a surface has no boundary, we say it is a *closed surface*.

An *orientation* of a surface at a point is a choice of which direction is “clockwise” at that point. An orientation of an entire surface is a choice of an orientation at every point so that the orientations of nearby points agree. If there exists an orientation of a surface, we say that the surface is *orientable*.

Not all surfaces are orientable—sometimes there is no consistent way to choose an orientation at every point. The simplest example of such a surface is the Möbius strip. Figure 4 shows why the Möbius strip isn’t orientable. Once you choose an orientation at a point, the local consistency condition forces the orientation at all nearby points. You can thus “push” your orientation around your surface to define what it must be everywhere. However, if you push it all the way around the Möbius strip, you get the opposite orientation at your original point of the one you started with, which shows you cannot consistently orient the surface.

If a surface is embedded in \mathbb{R}^3 , we note that an orientation is the same as a continuous choice of a unit outward normal vector at each point. To see this, notice that there are two choices for the outward normal direction at a point. Given a choice of outward normal, one can use the right-hand rule to choose an orientation. Similarly, one can select an outward normal vector given a choice of orientation.

There is a very simple classification of closed orientable surfaces up to homeomorphism.¹ We define the *genus-0* surface to be the sphere, the *genus-1* surface to be the torus, and the *genus- g* surface to be the “torus with g holes,” as shown in Figure 5. Now, the following theorem fully classifies closed orientable surfaces up to homeomorphism:

Theorem 2.2 *Every closed orientable surface is homeomorphic to the genus- g surface for some $g \geq 0$.*

Proof: This is a well-known classical result. For the proof, see [1]. \square

A surface is thus completely determined up to homeomorphism by its genus. For this reason, it will greatly facilitate our analysis to have a representation of a genus- g surface that is easier to work with. To this end, we construct a genus- g surface as follows. Start with a polygon with $4g$ edges, and label the edges as shown in Figure 6. Now, *identify* edges with the same letter. That is, if two edges have the same letter, we can pair off points on one edge with points on the other (using the direction of the arrows to determine which end of one edge matches up with which end of the other). Now, attach the surface to itself along these edges, treating each point on one edge as if it is touching the corresponding point on the other edge. It is not difficult to see, as shown in the figure, that these edge identifications yield the desired shapes. (Again, for the precise formulation of this construction, see [1].) By explicitly triangulating these polygons, we easily derive as a corollary that the Euler characteristic of a genus- g surface is $2 - 2g$.

We can now use the classification of closed oriented surfaces to classify oriented surfaces with boundary. The boundary of a compact 2-manifold with boundary is a compact 1-manifold without boundary. All such manifolds are disjoint unions of circles. We can now attach a disk along its boundary to each boundary circle of our surface. The result cannot have any boundary, and it is easy to see that the orientation of our original surface extends to the attached disks, so we now have a closed orientable surface with boundary. Applying Theorem 2.2, to this, we obtain:

Theorem 2.3 *Every orientable surface with boundary is homeomorphic to the genus- g surface with some collection of disjoint disks removed from it. Such surfaces are thus classified by their genus (which is defined to be the genus of the corresponding closed surface) and their number of boundary components.*

We can extend our $4g$ -gon representation of closed orientable surfaces to orientable surfaces with boundary by simply cutting little holes out of the interior of the polygon. As shown in Figure 7, this deformation-retracts onto a collection of circles attached at a point. The number of circles equals twice the genus plus the number of boundary components minus one. (Note that our surface must have nonempty boundary for us to perform this deformation retraction. There is no such deformation retraction for closed surfaces.)

Since Euler characteristic is unchanged by deformation retraction, we can compute it for all orientable surfaces with boundary by simply computing it for collections of circles attached at a point. Explicitly performing this computation and combining it with the above result for closed surfaces yields:

¹We shall restrict our attention to orientable surfaces. Classification results similar to the ones provided exist for nonorientable surfaces as well, but they are not needed and are therefore omitted.

Theorem 2.4 *An orientable surface S of genus g with n boundary components has $\chi(S) = 2 - 2g - n$.*

2.4 Knots and Links

Many of the arguments later in this paper draw their motivation from the theory of knots and links. Furthermore, our discussion of the boundary relies upon this theory explicitly. As such, we provide a very rudimentary introduction to knots and links. For a more complete introduction, see [3] for a very readable treatment, or [2] for a more advanced one.

Definition 2.5 *A knot in \mathbb{R}^3 is the image of a piecewise-linear embedding of the circle S^1 into \mathbb{R}^3 . A link is a union of nonintersecting knots. Two knots or links are considered isomorphic if they are the images of isotopic maps.*

We note that the knots that compose a link can be linked to one another so that you cannot pull them apart, as shown in Figure 8.

Intuitively, we can think of a knot as a piece of string in \mathbb{R}^3 with its ends glued together. Two knots are isomorphic if you can take one and pull the string (without cutting it or making it pass through itself) so that you get the other.

We can obtain a two-dimensional representation of a knot or link by projecting it into a plane and recording which strand passes on top at each crossing. (See Figure 9.) In order for this to be a good representation, we want our knot to be in *general position*: the projection should be injective at all but finitely many points, at each of which exactly two strands of the knot cross transversely. It is easy to see that any knot is isotopic to one that is in general position with respect to projection onto a given plane. (This depends essentially on the piecewise linearity of the embedding; the corresponding assertion for general topological embeddings of circles into \mathbb{R}^3 is false.)

The problem of classifying knots up to isotopy is a very hard one. Indeed, there is at present no polynomial-time algorithm to determine if two knots are isomorphic. In fact, there isn't even a polynomial algorithm to check if a knot is isomorphic to a simple, unknotted loop. Both problems have been shown to be decidable, however, using a tool from the theory of 3-manifolds called *normal surface theory*.

It is natural to ask which knots or links can be the boundary of an orientable surface. Perhaps surprisingly, the answer is that all of them can. Given a link L , a surface S with boundary L can be explicitly constructed using an algorithm known as Seifert's algorithm. A detailed explanation of this algorithm is provided in [2].

3 Definition and Classification up to Homeomorphism

We now define our primary objects of study:

Definition 3.1 *Let X be a connected orientable surface (as an abstract topological space), and let $f : X \rightarrow \mathbb{R}^3$ be a piecewise-linear embedding. We say that the pair (X, f) is a front-facing surface if we can choose an orientation on the image of f so that its outward normal vector has positive z -coordinate at all points.*

We shall occasionally abuse terminology and call a surface S in \mathbb{R}^3 front-facing if there exists a pair (X, f) such that $S = \text{Im}(f)$.

By the intermediate value theorem, we equivalently could mandate that the outward normal of the image of f have nonzero z -coordinate at all points. We also note that we lose no generality by requiring X to be orientable; had we not done so, the remainder of the definition would have forced it. More precisely:

Theorem 3.2 *If X is a surface (not necessarily orientable), and f is a piecewise-linear embedding, (X, f) is front-facing if and only if there is no point on the image of f at which a unit normal vector has z -coordinate equal to zero. In this case, we say that f realizes X as a front-facing surface.*

Proof: If (X, f) is a front-facing surface, clearly no unit-normal vector ever has z -coordinate equal to zero. For the converse, choose the unit normal vector with positive z -coordinate at each point of the image of f . This is a continuous choice of a normal vector, so the image of f (and thus X) is orientable by the remarks about orientability in Section 2.2, and one of the two orientations has this collection of normal vectors as its set of outward normals. \square

It is now natural to ask which orientable surfaces can be embedded in \mathbb{R}^3 as front-facing surfaces. We answer this question with the following theorem, which fully classifies front-facing surfaces up to homeomorphism:

Theorem 3.3 *Given an orientable surface X , there exists f such that (X, f) is front-facing if and only if X has nonempty boundary.*

Proof: We first show that an front-facing surface has nonempty boundary. To see this, let $S = \text{Im}(f)$, and consider the projection of S onto the xy -plane. Since the z -coordinate of a normal vector at a point is nonzero, the projection map will have nonzero Jacobian, so it will be a local homeomorphism. Since the projection of S will have nonempty boundary, this implies that S does as well.

For the converse, it suffices to prove that any surface X with one boundary component (i.e., a genus- g surface minus a single disk) can be realized as a front-facing surface. We can then realize surfaces with more boundary components by removing disks from X and restricting f to the result.

Let X_g be a genus- g surface minus a disk. To construct this, we start with the representation of S_g as a $4g$ -gon. All of the vertices of the polygon are collapsed to a point when you identify the sides. We construct X_g by removing a neighborhood of this point, as shown in Figure 10. We can now create a surface homeomorphic to this one by starting with a $4g$ -gon and using strips to attach pairs of identified sides, as shown in Figure 11. This surface is front-facing, which completes the proof. \square

4 Classification up to Isotopy

The classification of front-facing surfaces up to isotopy is considerably more complex than the classification up to homeomorphism. Accordingly, our classification puts isotopy classes of front-facing surfaces into correspondence with relatively complicated objects. However, these objects render the structure of a front-facing surface much more transparent, which greatly aids in our understanding of its properties. Throughout this section, we shall work in the smooth category. All of the results hold in the piecewise-linear category as well, and the proofs carry over with only minor technical modifications.

The intuition behind our classification is that front-facing surfaces look like flat strips almost everywhere. There are finitely many places, however, where they instead look like an intersection of a collection of streets, as shown in Figure 12. Looking at these pictures, we see that most of

the information about the isotopy class of a surface is embodied by the isotopy class of a one-dimensional “spine” that lies inside of it, as shown in Figure 13. It will turn out, however, that isotopy of front-facing surfaces is slightly more restrictive than isotopy of spines. We will thus need to supplement our spine with some extra information in order to specify a unique front-facing surface up to isotopy.

We recall that a front-facing surface is a topological space X along with an embedding of X into \mathbb{R}^3 . We begin by constructing particularly nice representations of our abstract topological spaces. We shall then endow them with an additional structure called a *striation*.

To this end, we define an n -street intersection to be a small neighborhood of an intersection of n segments in the plane, as shown in Figure 14. Now take a $2k$ -street intersection, and pair off the streets by connecting them with strips, as shown in Figure 15. We claim that there exists a space of this type homeomorphic to any orientable surface with boundary.

To see this, note that the front-facing surfaces with one boundary that we constructed in the last section are of precisely this form. Furthermore, given a surface of this form, we can create a new surface of this form with one more boundary component by poking a hole out of one of the connecting segments, and stretching this hole so that the result is an intersection of two more streets, as shown in Figure 16.

Now, away from the street intersections, our surfaces consist of a center line with an interval attached perpendicularly to each point. At the street intersections, we can also decompose our surface as a central spine with a bunch of intervals coming out of it, although the structure is slightly more complicated. For concreteness, we let our intervals be from -1 to 1 with 0 lying on the spine. Both cases are shown in Figure 17. We can thus endow each of our model spaces with the structure of a central spine and an interval passing through each point on the spine. Every point on our surface can be described uniquely by specifying a point on the spine and a number in the interval $[-1, 1]$. We call this structure a *striation* of our surface. We can use the map f to put this same structure on the image of our surface in \mathbb{R}^3 . We also note that the spines of our surfaces are all collections of circles attached at a single point.

The next statement that we would like to make is that we can classify front-facing surfaces up to isotopy by the isotopy classes of their spines. Unfortunately, this isn't quite the case. For example, the two pairs of surfaces shown in Figure 18 each have isotopic spines but are not isotopic. These show the two types of problems that can occur:

1. We can rearrange the ordering of the edges around the center point by isotoping the spine, but we cannot do this by isotoping a surface.
2. Two surfaces can have the same spine but can have different numbers of “twists” in some of their circles.

However, if we don't allow the isotopy to modify a small neighborhood of the point where all of the circles meet, and we keep track of how many twists are in each circle, we shall show that no problems can occur. With this in mind, we define the objects that we shall use to classify our front-facing surfaces:

Definition 4.1 *Let f be an embedding of a collection of circles attached at a point into \mathbb{R}^3 , along with an even integer assigned to each circle. If f maps a small neighborhood of the point at which the circles attach to a collection of segments in the xy -plane that is centered at 0 , and has the segments separated by equal angles, we say f is a generalized knot. Two generalized knots are isomorphic if one can be isotoped into the other while holding a small region of the center point rigid, in such a way that the even integers assigned to the circles match up in the obvious fashion.*

The basic idea is that you can use the striations on a front-facing surface to “thin” it out so that it looks like a bunch of strips attached at a street intersection. These objects will then be classified by their center lines and the number of twists in each of the strips.

Theorem 4.2 *Isotopy classes of front-facing surfaces are in one-to-one correspondence with isomorphism classes of generalized knots.*

Proof: Let $S = (X, f)$ be a striated front-facing surface. The striation on X allows us to define the spine of S to be the spine of X along with the restriction of f to this spine. We say that S is *rigidified* if the spine of S is a generalized knot. It is not difficult to show that any surface is isotopic to a rigidified one, and if two rigidified surfaces are isotopic, they are isotopic through rigidified surfaces. We thus have that classes of rigidified surfaces up to isotopy through rigidified surfaces are in one-to-one correspondence with isotopy classes of surfaces.

We start to define a map Φ from the set of rigidified front-facing surfaces to the set of generalized knots by taking the spine of a surface. It remains to define the number of twists in each circle. We do this by detaching the portion of our surface that corresponds to the circle (under the striation) from the rest of the surface, thereby giving us something that is topologically an annulus. We define the number of twists for the circle to be the linking number of one boundary component of this annulus with its center line. (This is a standard definition. It is not difficult to see that this coincides with one’s intuitive notion of the number of twists in an annulus embedded in \mathbb{R}^3 . An important point is that it is invariant under isotopy.) This number will be even because our surface is orientable. We note that Φ is clearly well-defined as a map from isotopy classes of rigidified front-facing surfaces to isomorphism classes of knots.

In the opposite direction, we define a “thickening” map Ψ from the set of generalized knots to the set of rigidified front-facing surfaces as follows. We isotope our generalized knot K so that its projection into the xy -plane has only transverse intersections. By compactness, there is some ϵ so that we can replace K with an ϵ -neighborhood of K , and no new intersections occur. (That is, if we drew the projection of K with a marker of thickness 2ϵ , it would still look as if in general position.) We now define a striated surface S in \mathbb{R}^3 by letting the generalized knot be the spine, and making the interval through a point on the spine be a horizontal segment of length 2ϵ centered on the spine. Now take the portion of S corresponding to each circle of the generalized knot, cut it, twist it so that its twisting number is as specified, and reattach it. We will show in the next section that this sort of object can be isotoped so as to be front-facing.

It is not immediately obvious that Ψ is well-defined. We have to check that isomorphic generalized knots yield isotopic front-facing surfaces. To this end, let K and K' be isomorphic knots, and let S and S' be their respective thickenings. We can isotope S' so that its spine coincides with the spine of S . Small neighborhoods of the central points of S and S' can be taken to match up precisely. Now consider the portions S and S' corresponding to a specific circle in the spines, intersected with the complements of the small neighborhoods of the central points. Each of these is a strip. Their center lines match up, they have the same width, and their ends coincide. All such objects containing the same number of twists can be isotoped into one another while holding the ends and spines fixed. This thus shows that Ψ is well-defined.

It now remains to show that $\Phi \circ \Psi = \text{Id}$, and $\Psi \circ \Phi = \text{Id}$. The former is completely trivial: if you take a generalized knot K and thicken it, the spine of the resulting striated surface is K again by construction. For the latter composition, let S be a rigidified front-facing surface. Compressing along the striation allows us to isotope S into a new surface S' that coincides with $\Psi \circ \Phi S$ at the intersection of streets, and such that all of the strips attached to this intersection of streets are of the same uniform width. The spines of the strips in S' coincide with those in $\Psi \circ \Phi$, and

corresponding strips have the same number of twists. By the comment in the last paragraph, S' is therefore isotopic to $\Psi \circ \Phi$, as desired. \square

5 Generality of Front-Facing Surfaces

One might expect the constraint that a surface be front-facing to place stringent restrictions on the isotopy class of the surface. But in fact front-facing surfaces are not really simpler than general surfaces, for it can be shown that every orientable surface in \mathbb{R}^3 with boundary is isotopic to a front-facing surface in \mathbb{R}^3 . Here we indicate briefly the proof of this somewhat surprising fact.

We begin with the observation that an annulus with two twists and a front-facing figure eight, shown in Figure 19, are isotopic. The same is true if we cut a small chunk out of both shapes and constrain the ends not to move; so the doubly-twisted strip and the more complicated but front-facing strip in Figure 20 are isotopic through maps fixing the ends of the strips. By induction we can use an isotopy to eliminate any even number of twists in a strip, at the cost of making the shape of its projected image more complicated, and this isotopy can be performed using only space very near the strip, so as not to collide with any other objects in space.

Suppose we are given a strip, possibly twisted in a very complicated manner, whose ends are constrained not to move. The strip is probably not presented in a front-facing manner, but we can flatten it out, starting at one end of the strip, so that it is mostly front-facing, with any twists in the strip accumulating at the other end of the strip. If the number of twists turns out to be even, we can use the figure-eight trick to eliminate them, obtaining a front-facing presentation of the strip. (If the number of twists is odd, we can eliminate all but one, but we shall not need this.)

Now a general orientable surface in \mathbb{R}^3 is isotopic to an embedded image of one of our abstract model spaces constructed by piecing several ribbons together at one complex intersection, and we may rotate the image so that the intersection is front-facing. Using the preceding argument, we can flatten out each ribbon to face entirely forward except for a possible aggregation of several twists at one point in the ribbon. The number of twists in such an aggregation is necessarily even: if it were odd, then traversing the ribbon once would reverse a local orientation, contradicting the assumption that our surface is orientable. We can therefore use the figure-eight trick to make each ribbon entirely front-facing, resulting in a front-facing representative of the isotopy class of the surface, as desired.

6 Winding Numbers

Any front-facing surface is homeomorphic to one of the abstract models considered in section 3. If, however, we are given a concrete front-facing surface, it may not be obvious to which of the abstract models the surface is homeomorphic. For example, it is not immediately apparent that the surface shown below in Figure 21 is a torus with two open disks removed. In this section we shall show how the topological identity of a front-facing surface can be deduced from simple and mechanical computations involving the boundary of the surface.

6.1 Definition of the winding number

To state the main theorem of this section, we shall need a precise definition of the *winding number* of an oriented closed curve, which is informally the net number of counterclockwise rotations made in a traversal of the curve. For instance, we should like to say that the circle in Figure 22a winds once, while the double circle in Figure 22b winds twice. Note that the orientation of the curve

matters: the circle in Figure 22c looks like that in Figure 22a except that it is traversed in the opposite direction, but we say that it winds -1 times.

Fortunately, it is easy to give a precise definition of this notion because we are dealing with piecewise-linear curves, which are merely finite chains of line segments. Given a piecewise-linear curve γ , we may divide γ into a series of linearly parametrized line segments ℓ_0, \dots, ℓ_N . For each $0 \leq i \leq N$ the segment ℓ_i ends where ℓ_{i+1} begins (we interpret indices modulo $N + 1$, so that ℓ_{N+1} means ℓ_0), and we can define the *relative angle* $\angle(\ell_i, \ell_{i+1})$ to be the counterclockwise angle between the two segments at the intersection point, measured as a fraction of a complete rotation (for instance, a 90° turn in the counterclockwise direction gives a relative angle of $\frac{1}{4}$). This number may be positive, negative, or zero. For instance, the curve shown in Figure 23 turns in the counterclockwise direction at v_{01} but in the clockwise direction at v_{12} , while at v_{23} it does not turn at all. We have

$$\angle(\ell_0, \ell_1) = +\frac{1}{6}; \quad \angle(\ell_1, \ell_2) = -\frac{1}{12}; \quad \angle(\ell_2, \ell_3) = 0.$$

We must assume that the path never turns around at a point, as the curve $f(t)$ given by

$$f(t) = \begin{cases} (t, 0, 0), & \text{if } 0 \leq t \leq 1; \\ (1-t, 0, 0), & \text{if } 1 \leq t \leq 2, \end{cases}$$

does at $t = 1$, for it is not clear whether the relative angle at the vertex is $+\frac{1}{2}$ or $-\frac{1}{2}$. We will not define the winding number for such a curve. For curves γ that do not misbehave in this way, however, we can define the winding number $w(\gamma)$ as the sum of the relative angles at vertices, namely

$$w(\gamma) = \sum_{0 \leq i \leq N} \angle(\ell_i, \ell_{i+1}). \tag{1}$$

It is now easily verified that the curves in Figure 22 have the winding numbers claimed previously; for instance, the circle in Figure 22a has eight vertices, each with relative angle $\frac{1}{8}$.

6.2 Elementary properties of the winding number

In each of the examples in Figure 22, the winding number is an integer; but the definition (1), which involves a sum of fairly arbitrary real numbers, gives no indication that this should be true in general. But in fact $w(\gamma)$ is an integer for *any* closed piecewise-linear curve γ . Our first object in this section will be to prove this fact. We decompose γ as a circular chain of segments ℓ_i as in the previous section, and we continue to measure directed angles in units of counterclockwise rotations.

For any directed segment ℓ , we define an *absolute angle* $\angle\ell$ of ℓ to be a counterclockwise angle from east to the direction of the segment. We say “a” and not “the” because the angle is not unique; there is a smallest nonnegative absolute angle, but we could obtain a larger angle, or a negative angle, by introducing extra complete rotations in one direction or the other, as shown in Figure 24. Nevertheless, the possibility of adding or subtracting complete rotations is the only ambiguity in the definition of the absolute angle in the sense that any two absolute angles of ℓ differ by an integer.

Considering now the segments ℓ_i of γ , fix one choice of the absolute angle $\angle\ell_0$. Then the ambiguity in the absolute angles $\angle\ell_i$ for $1 \leq i \leq N$ can be eliminated by requiring that the differences $\angle\ell_i - \angle\ell_{i-1}$ should equal the relative angles $\angle(\ell_{i-1}, \ell_i)$ for $1 \leq i \leq N$ (it is easily seen that this stipulation leads to valid absolute angles).

Considering now the segments ℓ_i of γ , fix one choice of the absolute angle of ℓ_0 , denoted \angle_0 . Now if \angle_i is an absolute angle of ℓ_i , it is easy to see that

$$\angle_{i+1} := \angle_i + \angle(\ell_i, \ell_{i+1}) \tag{2}$$

is an absolute angle of ℓ_{i+1} (see Figure 25). There were many ways to choose \angle_0 , but once one is fixed, we obtain unambiguous absolute angles \angle_i for all $i \geq 0$ by inductive application of (2). Figure 26 shows an example of the calculation of the \angle_i starting from the choice $\angle_0 = \frac{1}{4}$.

In particular we obtain an absolute angle \angle_{N+1} . This is an absolute angle for $\ell_{N+1} = \ell_0$, possibly different from the absolute angle \angle_0 (as it is in Figure 26). We do know, however, that the difference $\angle_{N+1} - \angle_0$ of the absolute angles is an integer. But using (2) we see that

$$\angle_{N+1} - \angle_0 = \sum_{0 \leq i \leq N} (\angle_{i+1} - \angle_i) = \sum_{0 \leq i \leq N} \angle(\ell_i, \ell_{i+1}) = w(\gamma),$$

whence the winding number $w(\gamma)$ is an integer, as claimed.

This result is comforting, and it also leads to the important fact that the winding number $w(\gamma)$ is *invariant under piecewise-linear homotopy of γ* . For it is intuitive and can be proven (though we omit the unsightly details) that the winding number is continuous in the time variable of such a homotopy. But a continuous function on $[0, 1]$ that takes integer values must be constant, and so $w(\gamma)$ is the same after the homotopy as before.

We have defined the winding number for closed curves only, but it is useful to have an analogous notion for arbitrary curves. A piecewise-linear curve γ , not necessarily closed, is still representable as a sequence of segments ℓ_i for $0 \leq i \leq N$. Define the *internal winding number* $\tilde{w}(\gamma)$ by the rule

$$\tilde{w}(\gamma) = \sum_{0 \leq i < N} \angle(\ell_i, \ell_{i+1}). \tag{3}$$

This is like the definition (1) of the ordinary winding number, except that (3) lacks the final term $\angle(\ell_N, \ell_{N+1})$ appearing in (1)—that last term makes less sense for arbitrary curves because ℓ_N need not end at the beginning of ℓ_0 . Unlike the winding number of a closed curve, the internal winding number of a curve is typically not an integer. Note that the internal winding number does *not* specialize to the ordinary winding number if the curve happens to be closed; in fact, it is immediate from the definitions that for a closed curve γ , we have the relation

$$w(\gamma) = \tilde{w}(\gamma) + \angle(\ell_N, \ell_0).$$

Similarly, if a (not necessarily closed) curve γ can be represented as a curve γ_1 followed by another curve γ_2 as in Figure 27, the internal winding number $\tilde{w}(\gamma)$ is the sum of the internal winding numbers of γ_1 and γ_2 , *plus* the rotation angle between the end of γ_1 and the beginning of γ_2 . We shall use these relations to great effect in the next subsection.

It is useful to introduce the notion of a *chain* in order to treat multiple curves at once without cluttering the analysis. A chain is a finite formal sum $\sum_i c_i \gamma_i$, where the c_i are integers and the γ_i are piecewise-linear curves. This is essentially a convenient notation for a collection of several curves, with multiplicities and orientations recorded. The chain $\gamma_1 + \gamma_2$ represents the pair γ_1 and γ_2 ; the chain 4γ represents four copies of γ ; and $-\gamma$ represents the curve γ traversed in the opposite direction. If $\sum_i c_i \gamma_i$ is a chain with γ_i closed curves, we can define its winding number by the rule

$$w\left(\sum_i c_i \gamma_i\right) = \sum_i c_i w(\gamma_i),$$

and similarly we can define the internal winding number of any chain.

An important special case of a chain (indeed, the reason why we care about chains here) is the boundary ∂S of a front-facing surface S . This boundary is a disjoint union of sets S_i homeomorphic to circles. We can make each S_i into a closed path γ_i merely by specifying the direction in which the circle is to be traversed, which we do as follows. At every point of ∂S there is a normal vector \mathbf{z} pointing out of the projection plane, as well as an outward normal \mathbf{n} to S lying in the plane. The cross product $\mathbf{z} \times \mathbf{n}$ is then tangent to ∂S in the plane. Let the direction of this vector be the direction of motion at that point on ∂S . It is easily seen that this gives a consistent orientation to each S_i , and we realize the boundary ∂S as the chain $\sum_i \gamma_i$.

6.3 Relation to Euler characteristic

We shall apply the theory of winding numbers developed above to the boundary of a front-facing surface, which has the structure of a chain of closed curves as noted above. Specifically, we shall prove that for any front-facing surface S , the winding number $w(\partial S)$ of its boundary equals the Euler characteristic $\chi(S)$ of the surface. Orientable surfaces are classified up to homeomorphism by their Euler characteristics and the number of their boundary components; the latter measurement is easily taken, so the stated theorem enables the homeomorphism class of a front-facing surface to be determined exactly.

We begin by appealing to the homeomorphism classification of front-facing surfaces to represent S as a thickening of a finite graph G with vertex set V and edge set E , say, as shown (in a concrete example) in Figure 28. The boundary ∂S can be decomposed as the union (not disjoint) of a pair $\gamma_e^I, \gamma_e^{II}$ of paths for each edge $e \in E$, as shown. Now S admits a piecewise-linear deformation retraction onto G that deforms γ_e^I and γ_e^{II} onto e for each e . The deformation retraction is a homotopy equivalence, so $\chi(G) = \chi(S)$; moreover, the homotopy does not change $w(\partial S)$ by the homotopy-invariance of the winding number. Thus it suffices to prove that $w(\partial S) = \chi(G) = |V| - |E|$.

Now $w(\partial S)$ equals the sum of the internal winding numbers of the γ_i plus the rotation angles at the junctions of adjacent paths γ_i . These junctions occur only at the vertices of G , and at each $v \in V$ there is a number of such junctions equal to twice the indegree $\deg^+ v$ of the vertex. (Here we define the indegree to be one-half the number of self-loops at v plus the number of edges of G other than self-loops that end at v .) We denote these rotation angles by \angle_v^i ($1 \leq i \leq 2 \deg^+ v$) as in Figure 29. With this notation, we are to prove that

$$\sum_{e \in E} (\tilde{w}(\gamma_e^I) + \tilde{w}(\gamma_e^{II})) + \sum_{v \in V} \sum_{1 \leq i \leq \deg^+ v} \angle_v^i = |V| - |E|. \quad (4)$$

We note first that for each e the paths γ_e^I and γ_e^{II} both traverse e once, but in opposite directions. Therefore $\tilde{w}(\gamma_e^I) = -\tilde{w}(\gamma_e^{II})$, and the sum over e in (4) vanishes. To deal with the vertex terms, note that for $v \in V$ the quantities $\frac{1}{2} + \angle_v^i$ are the nonnegative angles bounded by cyclically adjacent segments at v (see Figure 30), whence we must have

$$\sum_i \left(\frac{1}{2} + \angle_v^i\right) = 1,$$

or

$$\sum_i \angle_v^i = 1 - \sum_i \frac{1}{2} = 1 - \deg^+ v.$$

Therefore we have

$$w(\partial S) = \sum_{v \in V} (1 - \deg^+ v) = |V| - \sum_{v \in V} \deg^+ v = |V| - |E| = \chi(S),$$

which was to be demonstrated.

As an example, consider the front-facing surface shown before in Figure 21. There are two boundary components, of which the outer loop winds once counterclockwise, while the inner winds -3 times counterclockwise. Hence the winding number of the boundary is -2 , and the Euler characteristic is also -2 . Filling in the two holes yields a closed surface of Euler characteristic 0 , which is a torus, so the mystery surface is a torus with two open disks deleted.

7 Cutting Surfaces into Disks

In this section, we present an algorithm for “cutting” a (not necessarily front-facing) surface so that it becomes topologically a disk. This is useful in several contexts, as many other algorithms in graphics can be applied more easily to disks than to more topologically complicated objects. Before we can present the algorithm, however, we must make explicit the notion of a cut. To do this, we shall first need to set forth a small piece of machinery called the *combinatorial closure*.

Recall that if Δ is a simplex in some simplicial complex X , all of the faces of Δ are simplices in X as well. We define a *pseudosimplicial complex* to be an object that satisfies all of the conditions of the definition of a simplicial complex except for this one.

Let C be a pseudosimplicial complex, and let Δ^k be a k -simplex in C . We can define the set of *missing ℓ -faces of Δ^k* to be the set of ℓ -dimensional simplices in the boundary of Δ^k that are not in C . Now, we can fill in a missing ℓ -face of Δ^k by attaching an ℓ -dimensional simplex to Δ^k and endowing it with the minimal consistent set of adjacency data. If we fill in every missing face of every simplex in C , the result is a simplicial complex \bar{C} , which we shall call the *combinatorial closure of C* . This process is shown in Figure 31.

Now let X be a triangulated surface, and let P be a subset of the 1-skeleton of X comprising the edges e_1, \dots, e_n . Let C be the pseudosimplicial complex that results from removing e_1, \dots, e_n from X , and let $Y = \bar{C}$. We say that Y is the result of *cutting X along P* . An example of this is shown in Figure 32.

Our goal is to cut a surface along a sequence of simple curves that are either closed or have endpoints lying in the boundary, so that the resulting object is topologically a disk. We would like to do this while making as few cuts as possible. For technical reasons, we shall allow ourselves to slightly refine our triangularization when necessary.

We note that cutting along a simple closed curve doesn’t change the number of faces, and it changes the number of vertices and edges by the same amount; it therefore doesn’t affect Euler characteristic. Cutting along a simple curve with its endpoints in the boundary, however, creates one more vertex than it creates edges, so it increases Euler characteristic by one. A surface of genus g with n boundary components has Euler characteristic $2 - 2g - n$, and a disk has Euler characteristic one. Since no cut can decrease Euler characteristic by more than one, we thus must make at least $2g + n - 1$ cuts. If our surface is initially closed, our first cut must be along a simple closed curve, so we must make at least $2g$ cuts. The algorithms presented below will achieve these lower bounds.

We first consider a surface S with $n > 0$ boundary components. We can decrease the number of boundary components by one by cutting along a path that connects a pair of disjoint boundary components. We do this $n - 1$ times, so that we are left with a surface with one boundary component. This reduces the problem to the case where $n = 1$. We note that these paths can be found efficiently, for example, by constructing and using a depth-first tree of the 1-skeleton whose root is a vertex on the boundary. The total running time to construct this tree and use it to construct all of the above paths is linear in the number of simplices in our triangulation.

Let T be the closed surface that results from attaching a disk D along the boundary of S . We recall from Section 2.2 that if we puncture T , it will deformation-retract onto a collection of circles attached to one another at a point. The intersection of these circles with S yields a collection of segments that are in some sense the essential ones in S . Cutting along these will yield a disk. The mathematically inclined reader may find a more precise explanation of this in the remark at the end of this section.

We now describe an algorithm for computing these circles in T . We start by removing some triangle from T in order to puncture it. This creates a surface with boundary. Now choose some triangle Δ that shares an edge with the boundary. Remove the intersection of Δ with the boundary, and then remove the 2-simplex Δ . (See Figure 33.) We note that this is a deformation retraction. If we now repeat this process until there are no triangles left, what remains is a graph. Possibly refining our simplicial structure if necessary, we may arrange that this graph is homotopic to a collection of circles that only intersect at a single point in D , as shown in Figure 34. Taking the intersection of these circles with S yields a collection of segments s_1, \dots, s_{2g} , each of which has its endpoints on ∂D . These segments are the “essential” segments for which we were searching. We now cut along these segments to obtain a new surface Z .

Theorem 7.1 *Z is topologically a disk.*

We note that this theorem establishes the correctness of our algorithm. Our algorithm achieves our lower bound on the number of cuts, and it runs in time that is linear in the number of simplices in S .

Proof of Theorem 7.1: It suffices to show that Z is connected and has Euler characteristic one. Since each cut increases Euler characteristic by one, and we made $\chi(S) - 1$ cuts, we know that Z has Euler characteristic one, so we just need to show it to be connected. This follows rather easily using homology theory from the fact that our cuts form a collection of “essential” curves that is minimal in an appropriate sense. We make this slightly more precise in the remark at the end of this section. \square

Now suppose S is a closed surface. We puncture it and compute the graph onto which it deformation-retracts, as above. We then cut along one simple closed curve in this graph. It is not hard to see that this results in a connected surface R of genus $g - 1$ with one boundary component, to which we can now apply the above algorithm. We note that the graph onto which S deformation-retracts can be directly used in the application of our cutting algorithm to R , so this algorithm has almost exactly the same running time as the algorithm for cutting a surface with nonempty boundary.

Remark for the mathematically inclined: The “essential” curves discussed in this section are nontrivial elements of $H_1(S, \partial S)$. Since $T \cong S/\partial S$, the excision theorem tells us that the push-forward along the quotient map is an isomorphism from $H_1(S, \partial S)$ to $H_1(T)$. When you puncture T , it deformation-retracts onto a wedge sum of circles that form a basis for its first homology. The algorithm computes these circles, and then it finds a collection of elements of $H_1(S, \partial S)$ that map to them under the push-forward isomorphism. The proof that the result of cutting S along s_1, \dots, s_{2g} is connected uses just that the s_i form a basis of simple disjoint curves for $H_1(S, \partial S)$. If such a collection separated the surface into two components, one could show that the boundary of one of the components would represent a nontrivial sum of the the s_i in $H_1(S, \partial S)$, which would contradict that the s_i form a basis.

8 Conclusions

Our results are a mix of good and bad news. On one hand, we have deflated all hopes that the topology, whether up to homeomorphism or up to isotopy, of front-facing surfaces might be radically simpler than the topology of arbitrary surfaces because of the existence of a front-facing presentation. The homeomorphism type of a front-facing surface is not greatly restricted because we have shown that every abstract orientable surface with boundary is realizable as a front-facing surface. Moreover, we have shown that every orientable surface with boundary in \mathbb{R}^3 is isotopic to a front-facing surface; in light of Seifert's theorem that every link is the boundary of some orientable surface in \mathbb{R}^3 , this shows that the isotopy classification of front-facing surfaces is at least as complicated as the analogous classification of links, and mathematicians do not fully understand the latter problem at present. On the other hand, our isotopy classification of front-facing surfaces by their spines also shows that front-facing surfaces are not substantially more complicated than links, and our algorithms show that many analyses on front-facing surfaces involve only a reasonable amount of straightforward computation.

References

- [1] James Munkres. *Topology*. New Jersey: Prentice-Hall, Inc., 2000.
- [2] Dale Rolfsen. *Knots and Links*. Houston: Publish or Perish, 1990.
- [3] Colin Adams. *The Knot Book: An Elementary Introduction to the Theory of Knots*. New York: W.H. Freeman, 1994.

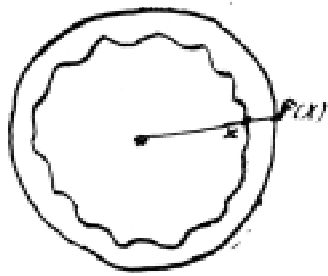


Figure 1

$(\sum \chi = 0? - \sum \chi(p))$ excised

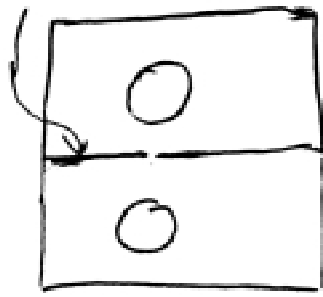


Figure 2

Wanted to do something that aren't simple complexes.

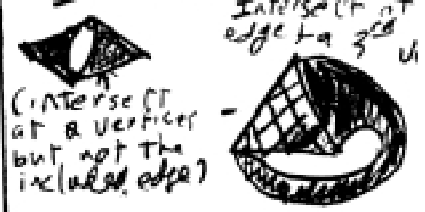


Figure 3

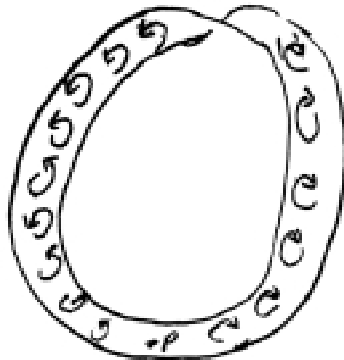


Figure 4

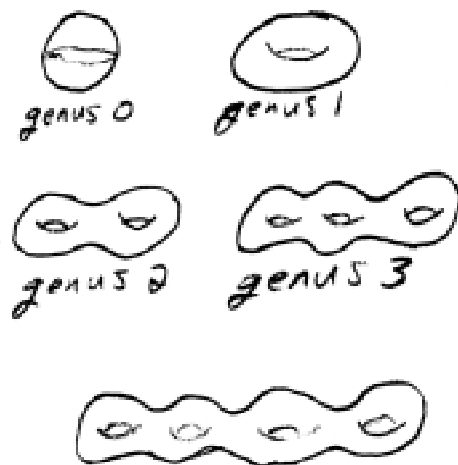
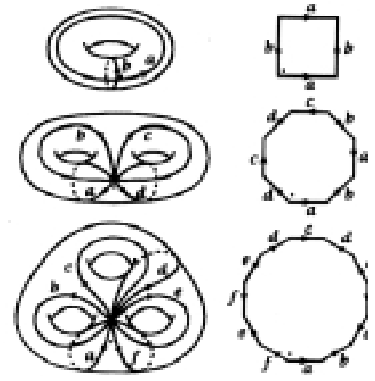
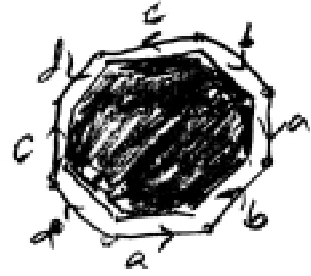
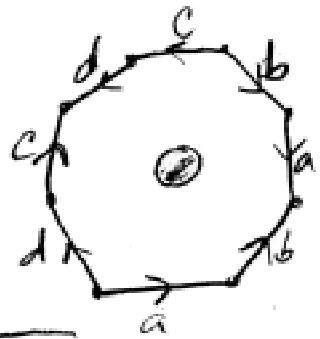


Figure 5



(From Algebraic Topology by Allen Hatcher.)

Figure 6



(performing the identification)

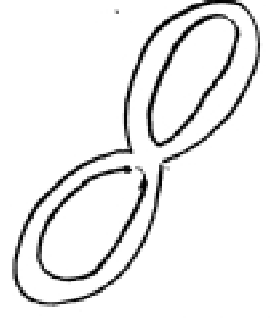
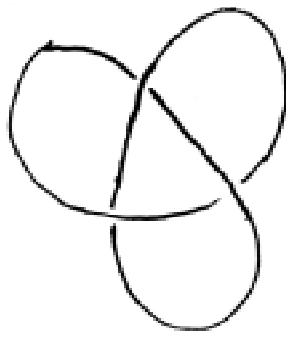
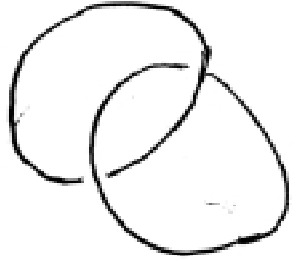
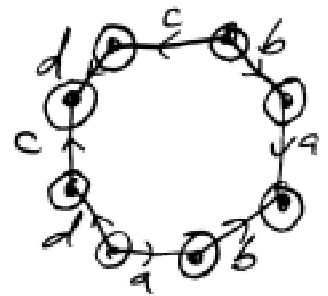


Figure 7



Remove the intersection of the circles with the polygon



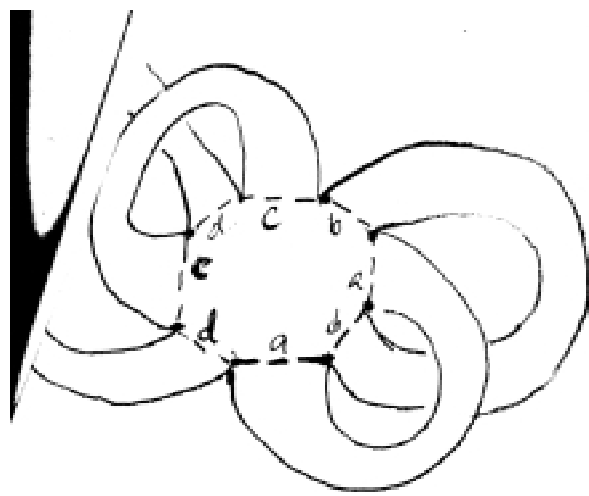


Figure 11



Figure 12

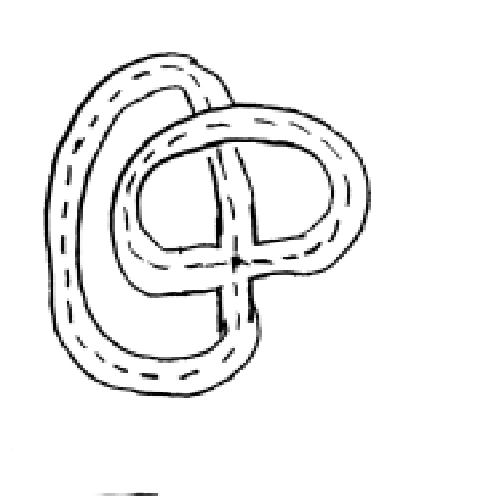


Figure 13

Intersection of 3 segments

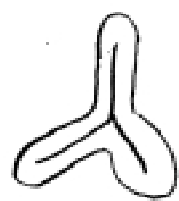


Figure 14

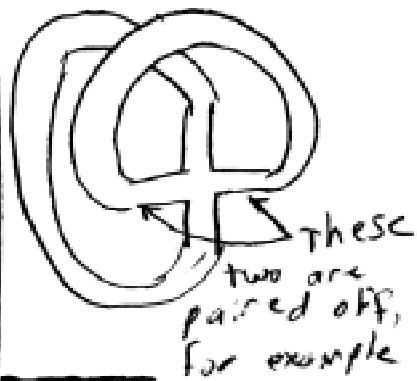


Figure 15



Figure 16

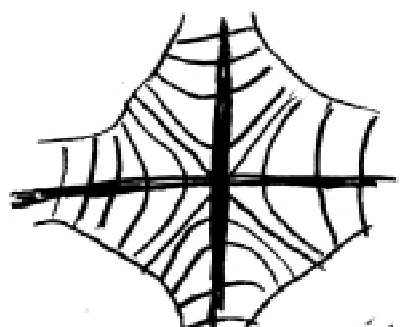
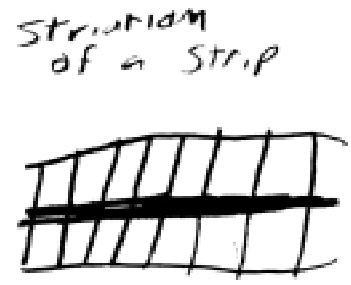


Figure 17: Striation of an intersection of streets



Striation of a strip

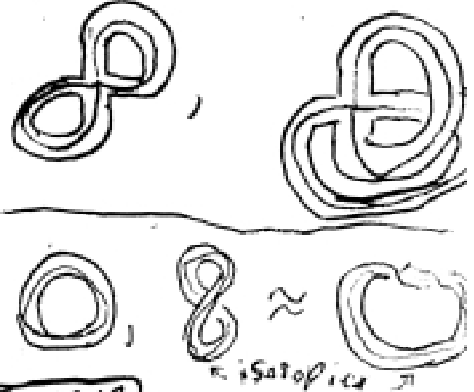
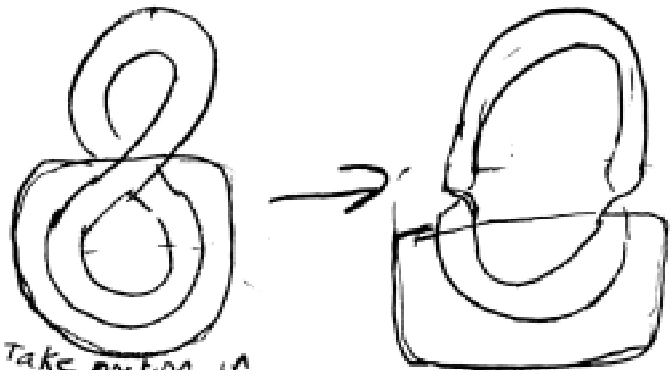
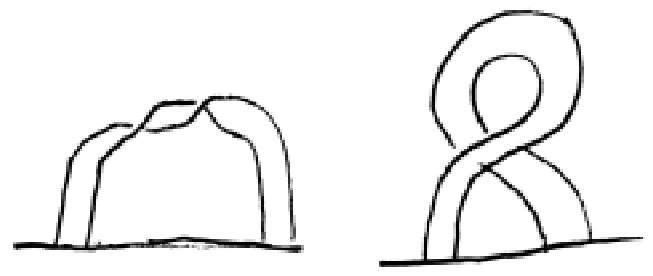


Figure 18



Take portion in box on twist around vertical axis



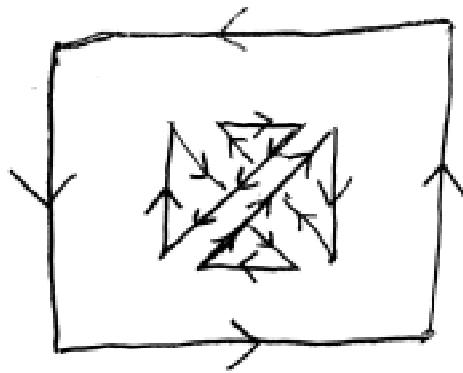


Figure 21

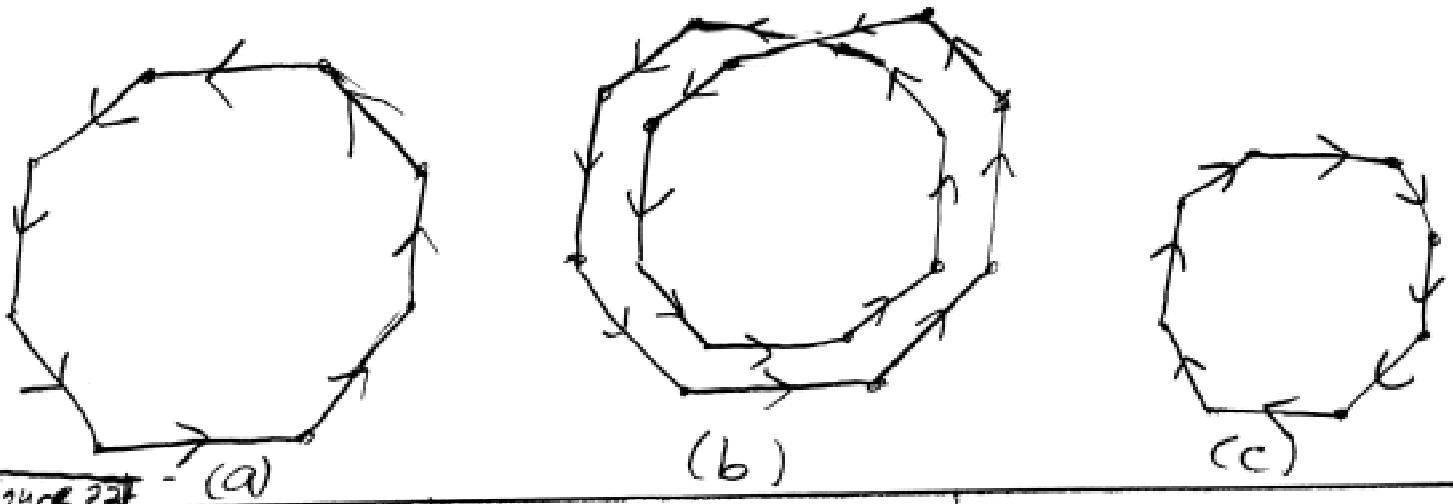


Figure 22

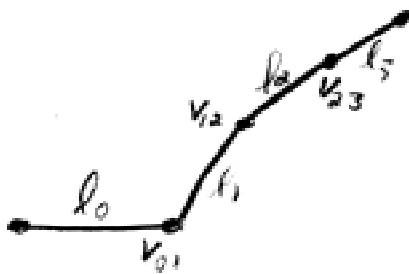


Figure 23

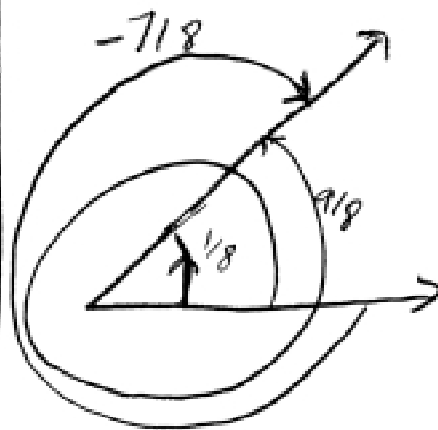


Figure 24

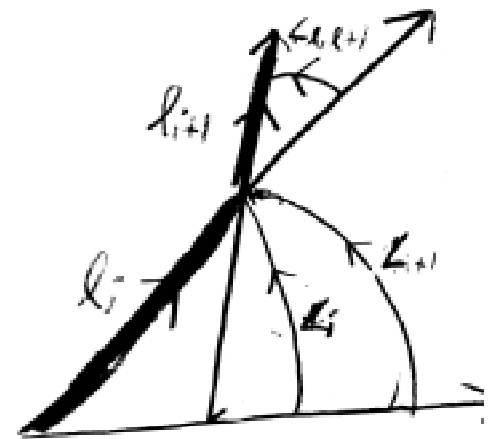


Figure 25

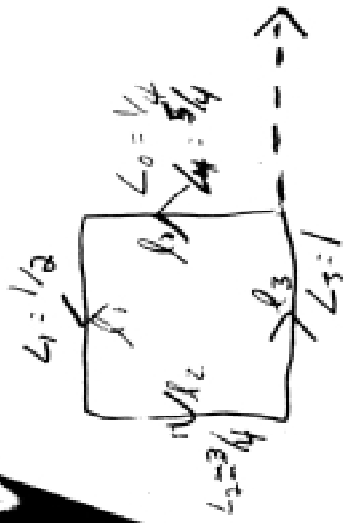


Figure 26

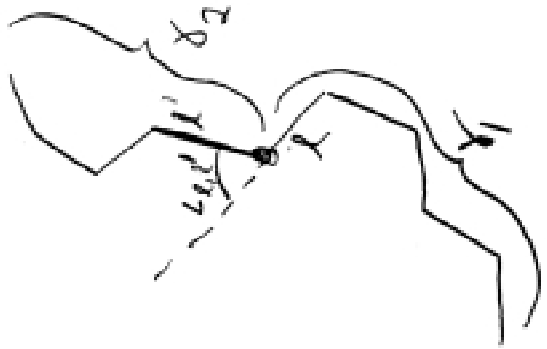


Figure 27

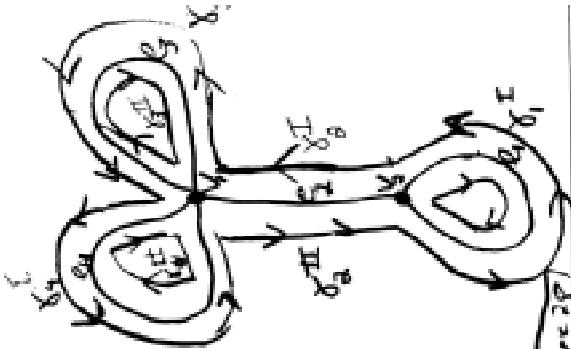


Figure 28

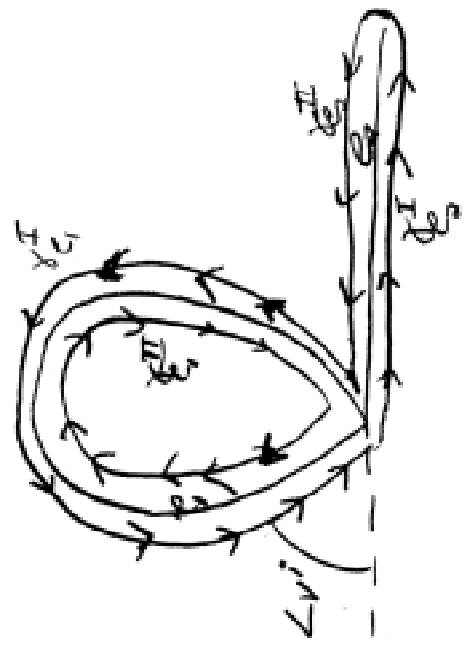


Figure 29

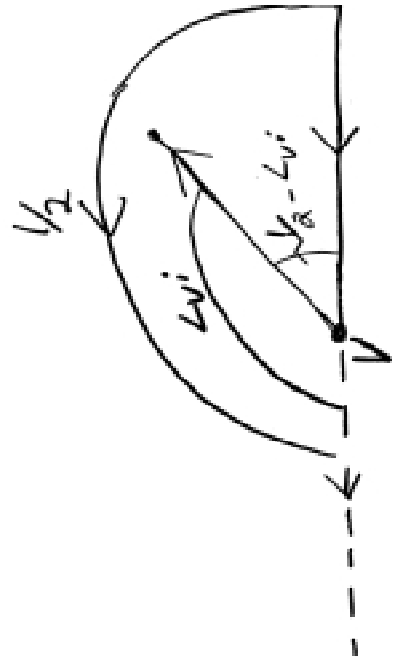


Figure 30

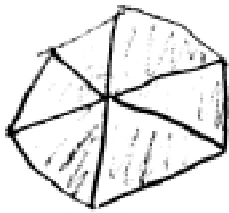
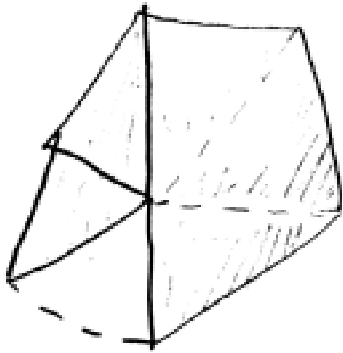


Figure 31

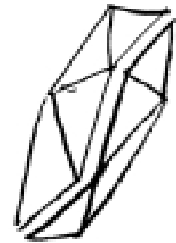
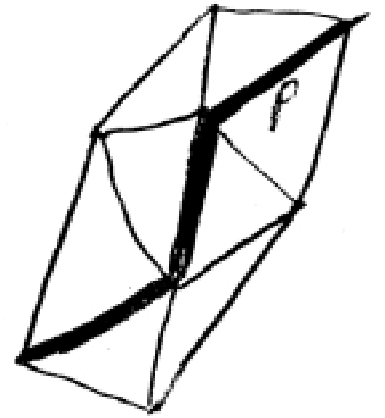


Figure 32

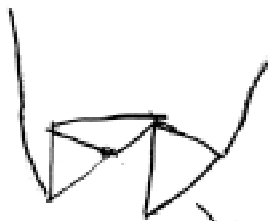
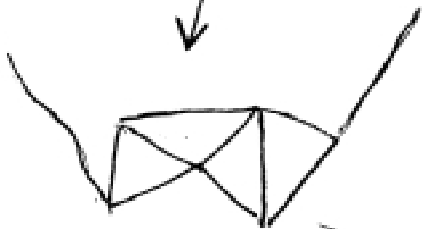
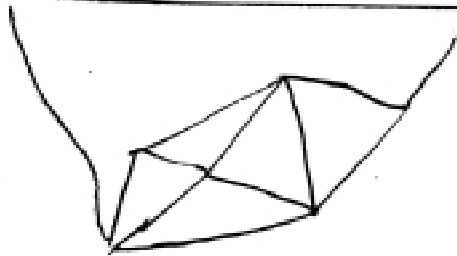
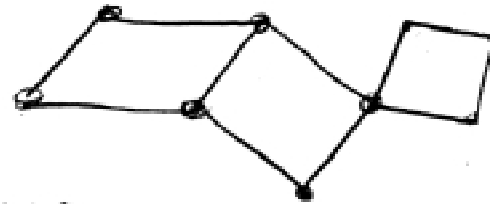


Figure 33



is homotopic to

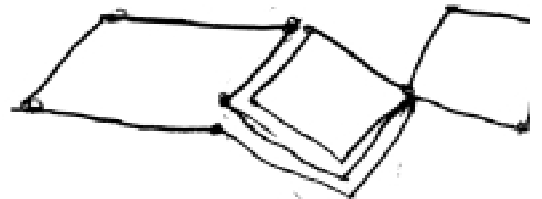


Figure 34